Intensity-Dependent Thermally Induced Nonlinear Optical Response of Graphene Oxide Derivative in Hydraulic Oil

Moein Golestanifar[a], Mohammad Ali Haddad[a,b,*], Amir Namiq Hassan[a,c], and Fatemeh Ostovari[a]

[a]Department of Physics, Yazd University, Yazd, Iran
[b]Laser Spectroscopy Research Laboratory (LSRL), Department of Physics, Yazd University, Yazd, Iran
[c]Department of Physics, College of Science, University of Sulaimani, Sulaymaniyah, Iraq

Corresponding author email: mahaddad@yazd.ac.ir

Regular Paper-Received: Received: Feb. 18, 2024, Revised: May 03, 2024, Accepted: May 04, 2024, Available Online: May 06, 2024,
DOI: 10.61186/ijop.17.2.121

ABSTRACT— The spatial self-phase modulation (SSPM) method was used to study the nonlinear optical responses of hydraulic oil containing dispersed nanosheets of reduced graphene oxide (rGO), hydroxylated rGO (rGO-OH), and carboxylated rGO (rGO-COOH). The intensity-dependent number of observed symmetric diffraction rings was analyzed to estimate the samples' thermally induced nonlinear refractive indexes and lead to estimated thermo-optical coefficients. Based on the observed symmetric diffraction rings, the nonlinear refraction coefficient and thermo-optical coefficient of samples were estimated to be in the order of magnitude of 10^{-6} cm^2/W and 10^{-2} K^{-1}, respectively. The results indicated that the presence of rGO derivatives significantly enhanced the optical nonlinearity of hydraulic oil.

KEYWORDS: Hydraulic oil, Nonlinear optics, Nonlinear refractive index coefficient, Spatial Self-Phase Modulation (SSPM), Thermo-optical coefficient

I. INTRODUCTION

The invention of the laser in 1960 led to significant advances in various scientific fields, mainly due to its unique properties, such as its remarkable intensity and coherence. Using lasers in laboratory research led to the discovery of nonlinear optics and related phenomena such as second and third harmonic generation. These developments established the basic principles of nonlinear optics [1, 2]. Many efforts have been made to study the effect of high-intensity laser light on the optical properties of various materials. The study of the interactions of lasers with multiple materials has led to an understanding of their nonlinear optical properties, including changes in refractive index coefficient, absorption coefficient, and polarization state. In recent years, nonlinear optics has become an important research area due to its wide range of applications in photonic devices [3,4]. The development of numerous technologies, such as ultrafast lasers, frequency combs, and optical parametric amplifiers, has been significantly assisted by nonlinear optics. Nonlinear optical materials enable advanced lighting functions such as all-optical switching, optical limiting, optical diodes, etc. The demand for materials with high nonlinear properties for many optical devices and applications has increased rapidly. Many researchers have worked to identify materials with high nonlinear optical responses due to their potential applications [5,6]. Analysis of the relationship between measurable macroscopic parameters and microscopic nonlinear optical properties of photonic materials defines the field of nonlinear optical material characterization [7, 8].

Different techniques such as four-wave mixing [9, 10], Z-scan [11, 12], and Spatial Self-Phase Modulation (SSPM) [13, 14] are almost known as conventional methods to study nonlinear optical behavior and measure nonlinear optical index. SSPM is a phenomenon that occurs when a laser beam interacts with a nonlinear medium, causing a spatially varying phase shift in the beam. The SSPM effect can be observed by forming self-diffraction ring patterns in the far field of the beam. The properties of these rings, including their quantity, morphology, and deformation, depend on various factors such as the sample's spatial orientation, the laser's intensity, and the geometric pumping mechanism [58]. Since it is a vital technique for determining the nonlinear optical properties of different materials, SSPM analysis has been observed on several materials and serves various objectives. For instance, this method has been used to analyze edible oils to determine the level of adulteration [15]. Furthermore, SSPM analysis has been employed to investigate the thermal convection phenomenon exhibited by a polymer called DAZA [16]. Moreover, SSPM studies have been used to determine the modes of orbital angular momentum using rubidium atomic vapor [17].

The nonlinear optical properties of two-dimensional (2D) materials, namely atomic layers of graphene oxide (GO) [18] and black phosphorus (BP) suspensions [19], have been studied in detail. These studies have provided valuable information about various material properties, including the number of layers, crystal orientation, presence of defects, and chemical dynamics [20-22]. Graphene has great potential in various areas where properties such as high strength, thermal stability, and chemical resistance are required. Recent studies have focused on the nonlinear optical properties of graphene-based materials. Many nonlinear optical phenomena such as saturable absorption, reverse saturable absorption, two-photon absorption, and optical confinement have shown promising results for these materials, which include pure graphene, graphene oxide, and graphene hybrids [59]. Studying the nonlinear optical properties of graphene and its derivatives is crucial for evaluating its potential use in optoelectronic devices. Many scientific works have reported graphene's enhanced nonlinear optical properties and derivatives [23-26]. For example, the use of graphene oxide decorated with carbon dots (CDs-GO) [27], Cu_2Se/reduced graphene oxide (rGO) [28], reduced graphene oxide decorated with silver nanoparticles (Ag NPs/rGO) [29], and methylammonium lead bromide-graphene ($CH_3NH_3PbBr_3$-G) composites [30] have shown significant improvements in the nonlinear optical response of materials. These results indicate that graphene-based materials have considerable potential to improve the nonlinear optics of various photonic devices. This makes their use in ultrafast photonics and pulsed waveguide laser systems particularly interesting.

Hydraulic oils are critical in lubricating hydraulic components as they help minimize friction, prevent contamination, reduce wear, and prevent corrosion. Adding nanoparticles to hydraulic oil has been found to reduce friction and increase corrosion resistance, potentially leading to improved machine efficiency [31-33]. In recent years, several studies have been devoted to investigating the nonlinear optical properties of different types of oils, mainly using Z-scan and SSPM methods [34-37]. The investigation of the nonlinear characteristics of castor oil and a water-in-oil microemulsion film revealed a significant negative nonlinear refractive index. This indicates that the nonlinearity is caused by thermal effects [38-42]. Castor oil also exhibited spatial self-phase modulation, with the minimum power required to induce this effect decreasing with increasing sample length and laser wavelength near the absorption region of the medium. The presence of gold nanoparticles in castor oil increases the nonlinear refractive index, especially near the plasmon resonance of the nanoparticles. The observed slow time response of nonlinearity suggests that thermal effects significantly influence. The phenomenon of optical nonlinearity in a water-in-oil microemulsion film was observed and studied using self-phase modulation [43-46]. The influence of the

composition of the microemulsion using oils with different dielectric constants on the nonlinear optical properties of Alizarin Red S and was investigated. It was found that the dielectric constants of the media on the second and third order nonlinearities have a significant effect on the NLO response [47]. The effect of different nanometer-sized droplets on the improvement of the nonlinear optical properties of an aqueous solution was also investigated in detail [48-50]. In this study, we investigate the influence of graphene oxide derivatives on the nonlinear optical response of hydraulic oil by using various functionalized reduced graphene oxide nanoparticles which include reduced graphene oxide (rGO), hydroxylated reduced graphene oxide (rGO-OH), and carboxylated reduced graphene oxide (rGO-COOH). For this purpose, the thermally induced nonlinear refractive index (n_2) and the estimate of the thermo-optical coefficients (dn/dT) for different samples were measured using a 532 nm continuous wave laser. The experimental observations show the significant influence of graphene nanoparticles on the nonlinear optical behavior of utilized hydraulic oil. The study used the popular SSPM method, known for its simplicity and accuracy in studying nonlinear media's nonlinear responses.

II. EXPERIMENTAL AND METHODS

Self-phase modulation is a nonlinear optical phenomenon in which the intensity of a Gaussian laser beam causes changes in the refractive index of the optical material through which it travels. This effect induces various nonlinear optical phenomena that result in a non-uniform radial phase shift within the material. Consequently, this radial phase shift leads to spatial changes in the refractive index, forming concentric rings in the far field. Due to the even or odd nonlinear phase difference, these rings arise from constructive (bright rings) and destructive (dark rings) interference. Analyzing the aforementioned concentric ring patterns provides insights into the nonlinear optical properties of the samples.

According to previous studies, the emergence of SSPM phenomena is believed to be influenced by a variety of factors, including molecular reorientation [51, 52], third-order susceptibility effects [13, 53], and thermo-optical effects [50-54]. When SSPM arises from nonlinear media's electronic or molecular orientation, it is related to the real part of the third-order electronic susceptibility [55]. It is known that using a continuous wave laser does not provide enough time for the system to relax thermally. Therefore, the observed diffraction ring pattern cannot be attributed to the nanomaterial's intrinsic electronic nonlinear optical effect in the solvent. As described in [56], When SSPM is caused by thermal effects, the relationship between the nonlinear optical refractive index, n_2 and third-order susceptibility, χ^3 is often incorrect.

Nanomaterials play a role here by absorbing laser light and converting it into heat in the sample. Due to the intensity of the laser beam, this process leads to localized heating and thermal effects in the medium. The nonlinear optical refractive index changes significantly in optical materials with a high thermo-optical coefficient [57, 58]. The relative phase shift $\Delta\phi(r)$ of a cylindrically symmetric Gaussian beam propagating in a liquid sample is approximated by[59]:

$$\Delta\phi(r) = \Delta n \exp\left(-\frac{2r^2}{a^2}\right) kL_{eff} = \Delta\phi(0)\exp\left(-\frac{2r^2}{a^2}\right) \quad (1)$$

where $\Delta nkL_{eff} = \Delta\phi(0)$, Δn is the average on-axis refractive index change, k is the wave vector, L_{eff} is the sample's effective length, a is the constant that gives the spread of phase shift, and $\Delta\phi(0)$ is the corresponding phase shift. The following equation shows the correlation between the number of observable rings, N and the phase shift of $\Delta\phi(0)$ [60]:

$$\Delta\phi(0) \cong 2\pi N \quad (2)$$

In other words, the correlation between Δn attributed to thermal effects (Δn_{th}) and incident on-axis laser intensity, $I(0)$, may be expressed as follows [54]:

$$\Delta n_{th} = n_{2,th} I(0) \quad (3)$$

where $n_{2,th}$ is the effective nonlinear coefficient and the subscript "*th*" refers to its thermal origin. Thus, by using Eq. (2) and the relationship between the number of concentric rings and the incident beam intensity, $I(0)$, we can derive an estimation for the $n_{2,th}$ based on the nonlinear phase shifts, which are expressed as:

$$\Delta\phi(0) = \Delta n_{th} k L_{eff} = n_{2,th} I(0) k L_{eff} = 2\pi N \quad (4)$$

As a result, the nonlinear refractive index $n_{2,th}$ is given by [54, 58]:

$$n_{2,th} = \frac{\lambda}{L_{eff}} \frac{N}{I} \quad (5)$$

As mentioned, the variable N represents the number of SSPM fringes and λ denotes the wavelength of the laser used in the experiment. Also, $I = \frac{2P_{av}}{\pi\omega_0^2}$ represents the intensity of the laser beam. The intensity is calculated based on the beam waist (in our work ω_0 was 110 μm) of the laser at the focal point. Assuming a reasonably collimated beam passing through the sample and a nearly constant transversal area within the cuvette length, L_{eff}, can be determined by the linear absorption, α_0, of the samples and the length of the sample's cuvette, L, [54]:

$$L_{eff} = \frac{(1-e^{-\alpha_0 L})}{\alpha_0} \quad (6)$$

Furthermore, for thermal nonlinearity, the change in the on-axis nonlinear index is expressed by[59]:

$$\Delta n_{th} \cong \frac{\partial n}{\partial T} \frac{I\alpha_0\omega_0^2}{4\kappa} \quad (7)$$

where, κ is the thermal conductivity constant of the samples and $\partial n/\partial T$ is the thermo-optical coefficient. From Eq. (5), the value of $\frac{\partial n}{\partial T}$ can be estimated using the following equation [54, 58]:

$$\frac{\partial n}{\partial T} = \frac{4K}{\alpha_0 \omega_0^2} n_{2,th} \quad (8)$$

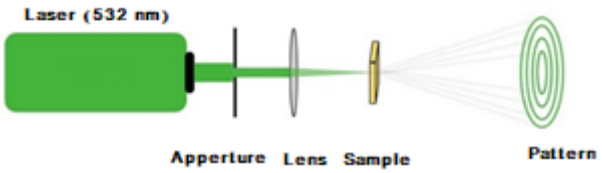

Fig. 1. SSPM experimental setup for studying nonlinear optical response.

Figure 1 depicts the experimental setup used to observe the SSPM. Our experiment used a continuous-wave (CW) laser with a wavelength of 532 nm. A converging lens with a focal length of 15 cm was also used to focus the incident beam onto the samples inside a 1 cm quartz cuvette. A Canon camera (X50) captured images during the experiment. The nanoparticles used in this study were obtained from "Nano Sanjesh" Company-Iran, while the hydraulic oil was provided by "Behran Oil" Company-Iran. The dispersion process involved ultrasonic mixing the nanoparticles with the hydraulic oil for two hours, at concentrations of 40, 160, and 440 *μg/cc*.

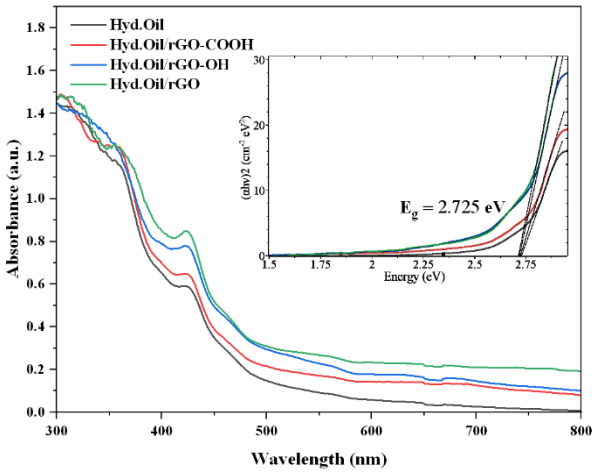

Fig. 2. Absorbance spectrum of hydraulic oil alone and with 440 μg/cc concentration of rGO, rGO-OH, and rGO-COOH nanosheets. The inset figure shows the derived Tauc diagram.

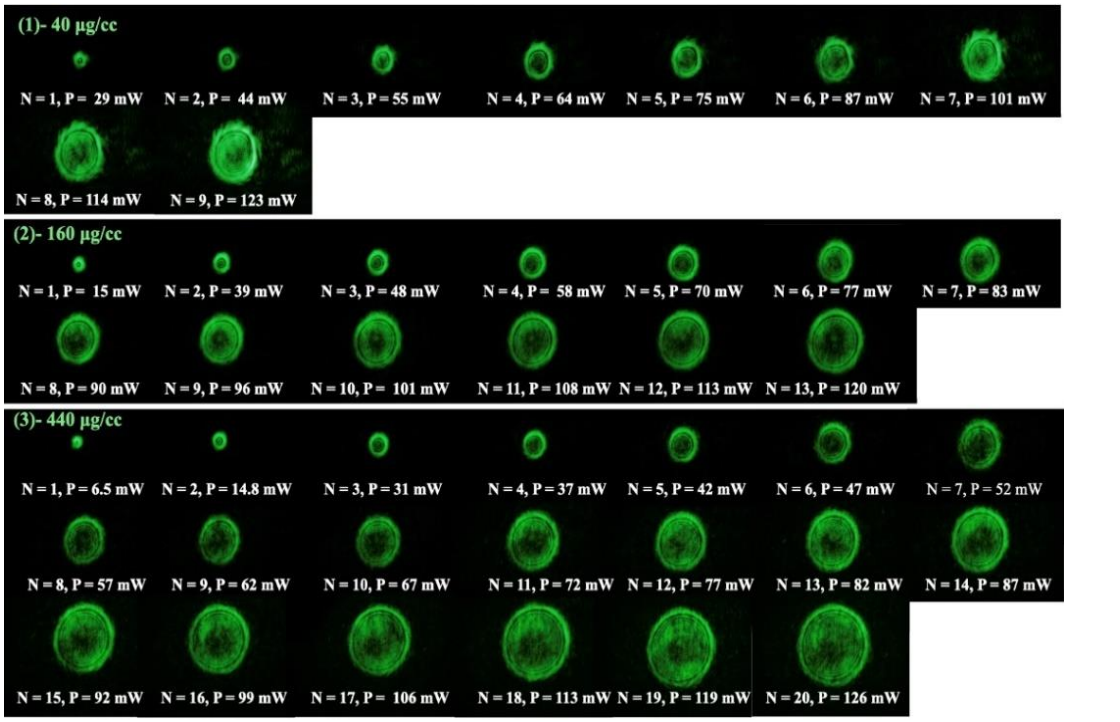

(a)

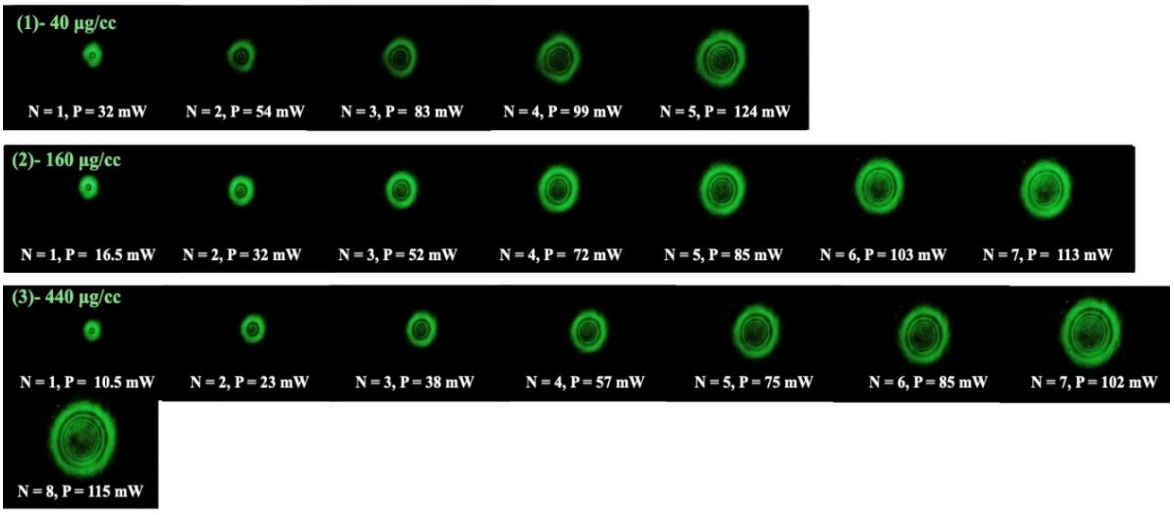

(b)

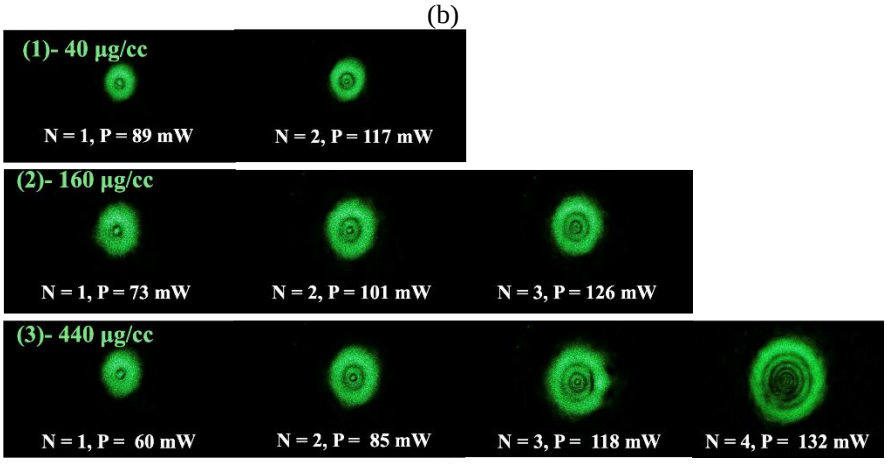

(c)

Fig. 3. SSPM diffraction ring patterns of hydraulic oil containing: (a) rGO, (b) rGO-OH, and (c) rGO-COOH in 40, 160, and 440 µg/cc concentration.

III. RESULTS AND DISCUSSION

The UV-Vis spectra of pure hydraulic oil and graphene oxide derivatives such as rGO, rGO-OH, and rGO-COOH in hydraulic oil at the maximum produced concentration of 440 µg/cc are shown in Fig. 2. As already mentioned, the thermally induced nonlinear optical behavior is directly related to the absorption properties of the medium at the excitation wavelength. Remarkably, no SSPM fringes were observed, attributable to the low absorption coefficient of pure hydraulic oil at the wavelength of 532 nm. Also, samples with a higher linear absorption coefficient absorb more light at a given wavelength and experience more substantial thermal effects. The Tauc diagram in Fig. 2 shows that the band gap energy values of E_g=2.7 eV for different graphene oxide derivatives in hydraulic oil with the same concentration are very close to each other. This confirms that the observed diffraction ring pattern cannot be attributed to the intrinsic electronic nonlinear optical effect of the nanomaterial in the solvent.

As shown in Fig. 2, the sample of rGO in Hydraulic Oil with the concentration of 440 µg/cc had a higher absorption coefficient (0.64 cm^{-1}) than rGO-OH and rGO-COOH in the region of interest at 532 nm. Due to the higher absorption coefficient of the sample containing rGO nanoparticles, the thermal effects of the medium are stronger, and this sample was expected to have a more extensive thermally induced nonlinear refractive index than rGO-OH and rGO-COOH in hydraulic oil samples. Consequently, the number of apparent SSPM ring patterns for rGO, rGO-OH, and rGO-COOH differs in hydraulic oil samples with the same beam intensity.

Figures 3(a) to 3(c) show the observed SSPM ring patterns for rGO, rGO-OH, and rGO-COOH in hydraulic oil samples at different concentrations by varying the incident beam power. As shown in Fig. 3, the number of observed rings increased as the power was increased. For the samples with the higher concentration of nanoparticles, the growth of ring formation was higher than for the samples with lower concentration. Their absorption coefficients were also relatively low at the laser wavelength used. This indicates that the thermally induced effect is dominant in forming SSPM rings for all samples. The number of ring patterns generated increased linearly with the intensity of the laser beam. As a result, the value of $n_{2,th}$ for each sample can be estimated for calculation using Eq. (5).

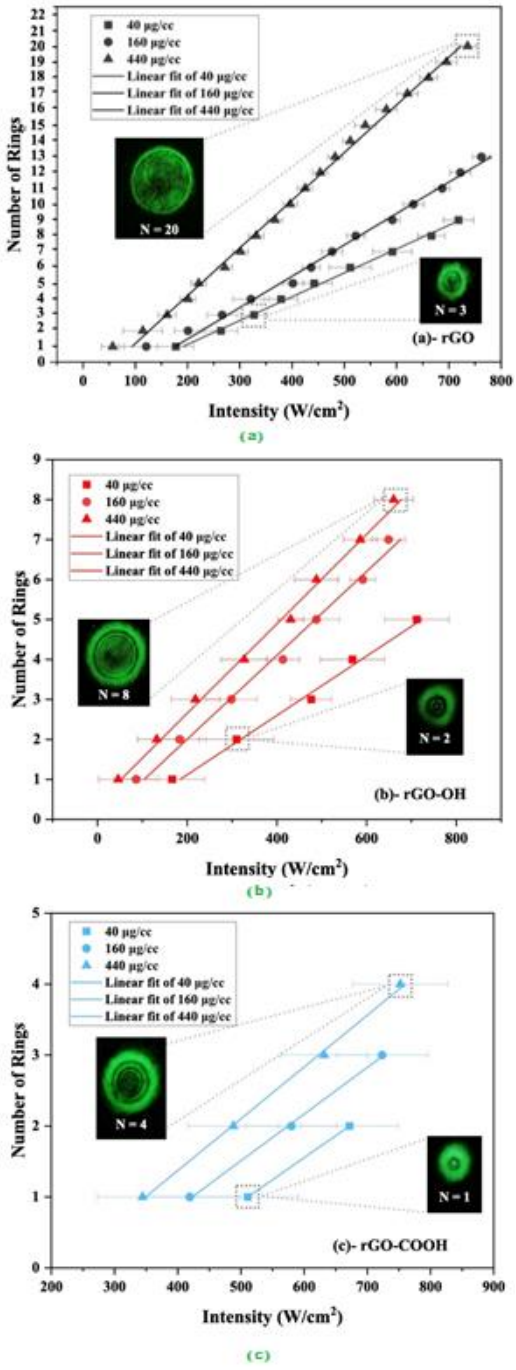

Fig. 4. Number of rings as a function of incident intensity for 40, 160, 440 µg/cc concentration of: (a) rGO, (b) rGO-OH, and (c) rGO-COOH nanosheets in hydraulic oil.

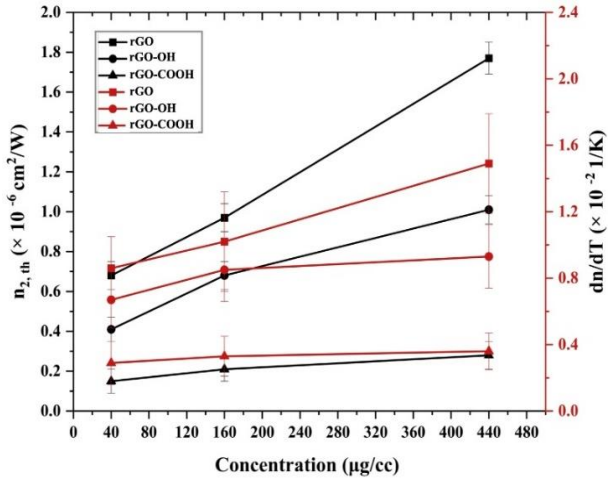

(a)

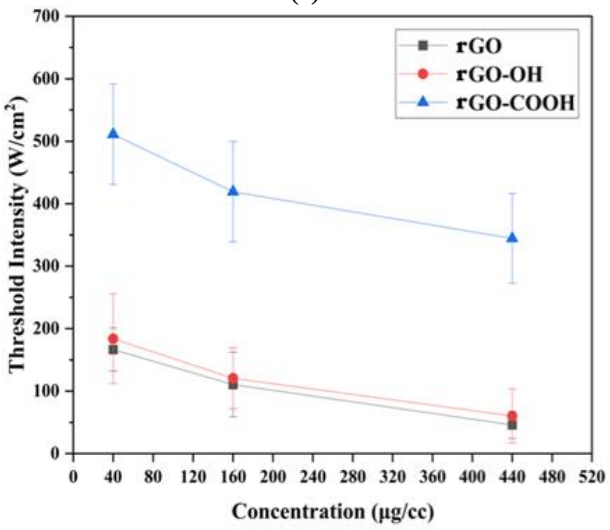

(b)

Fig. 5. (a) Nonlinear refractive index & thermo-optical coefficient, (b) Threshold intensity.

Figures 4(a) to 4(c) show the observed ring number (N) versus the beam intensity (I) for all samples. The dots represent experimental data with error bars, while the solid lines represent linear fits. Based on the experimental data, the value of the thermally induced nonlinear refractive index was estimated for all samples. Table 1 shows all samples' measured values and $n_{2,th}$ values that agree with the expected values for thermally induced NLO parameters [55]. Using the same approach described in [54], [57], the error in calculating $n_{2,th}$ was considered as the error of N/I together with the error in calculating L_{eff}, which corresponds to the error of the absorption coefficient. We chose a tolerance of 5% in estimating the absorption coefficient for each sample at 532 nm based on the technical specifications of the spectrometer used to evaluate the thermo-optical coefficient of the samples in this work, it is necessary to know the thermal conductivity (κ) for each sample of rGO, rGO-OH, and rGO-COOH in hydraulic oil separately. Since the exact value for each sample with different concentrations was not available, we fixed the thermal conductivity of hydraulic oil (κ=0.15 W/mK) reported in [60] to evaluate the variation of the thermo-optical coefficient of all samples at different concentration. As expected, in Fig. 5(a), the variation of the thermo-optical coefficient follows the variation of $n_{2,th}$ estimated for the samples. The measured values of the thermo-optical coefficient of the samples are listed in Table 1. It was found that the nonlinear refractive index values for different samples did not correlate with the band gap energy calculated for different graphene oxide derivatives in hydraulic oil and their intrinsic third-order susceptibility factor, χ^3. This confirms that the observed nonlinear optical behavior in our samples was caused by thermal effects.

In our experiment, we found that each sample had a specific threshold intensity (I_{ths}), which reflects the minimum intensity required to detect the first SSPM ring. An increase in the concentration of rGO, rGO-OH, and rGO-COOH in the samples decreased the threshold power, leading to an enhanced nonlinear optical response. Figure 5(b) illustrates the correlation between the threshold intensity and the quantity of rGO nanoparticle derivatives in the hydraulic samples. The measured values of the nonlinear optical parameters are provided in Table 1. Consistent with our SSPM results, these values are correlated with the concentration of rGO nanoparticle derivatives in hydraulic samples, indicating that a higher concentration of rGO nanoparticles results in increased optical nonlinearity. Furthermore, the variation of $n_{2,th}$ and $\partial n/\partial T$ in different concentrations suggests that thermal is the dominant effect in the studied SSPM phenomenon.

Table 1. Measured nonlinear optical parameters of samples.

Sample	*Conc.* ($\mu g/cc$)	α_0 (cm^{-1})	L_{eff} (cm)	N/I (cm^2/W)	$n_{2,th}\times10^{-6}$ (cm^2/W)	$dn/dT\times10^{-2}$ ($1/K$)
Hyd.Oil + rGO	40	0.42 ± 0.02	0.82 ± 0.04	0.010 ± 0.002	0.68 ± 0.07	0.86 ± 0.19
	160	0.51 ± 0.03	0.78 ± 0.04	0.014 ± 0.004	0.97 ± 0.07	1.02 ± 0.30
	440	0.64 ± 0.03	0.74 ± 0.03	0.025 ± 0.004	1.77 ± 0.08	1.49 ± 0.30
Hyd.Oil + rGO-OH	40	0.34 ± 0.02	0.85 ± 0.04	0.007 ± 0.0005	0.41 ± 0.06	0.67 ± 0.17
	160	0.43 ± 0.02	0.81 ± 0.04	0.011 ± 0.0007	0.68 ± 0.07	0.85 ± 0.19
	440	0.59 ± 0.03	0.76 ± 0.04	0.014 ± 0.009	1.01 ± 0.07	0.93 ± 0.19
Hyd.Oil + rGO-COOH	40	0.28 ± 0.01	0.87 ± 0.04	0.003 ± 0.0007	0.15 ± 0.06	0.29 ± 0.13
	160	0.34 ± 0.02	0.85 ± 0.04	0.003 ± 0.0009	0.21 ± 0.06	0.33 ± 0.12
	440	0.42 ± 0.02	0.81 ± 0.04	0.004 ± 0.001	0.28 ± 0.07	0.36± 0.11

IV. CONCLUSION

In this paper, we utilized the SSPM technique to evaluate the nonlinear optical response of rGO nanoparticle derivatives, including rGO, rGO-OH, and rGO-COOH, in hydraulic oil samples. Considering that pure hydraulic oil did not exhibit any SSPM fringes in our experiments, it is essential to understand the source of SSPM in the presence of additional nanoparticles. When a focused laser beam was directed through samples of hydraulic oil containing dispersed nanosheets of rGO, rGO-OH, and rGO-COOH, it generated a distinct diffraction ring pattern in the far field known as the SSPM diffraction ring pattern. The primary scientific question is whether the phenomenon is caused by the intrinsic nonlinear refractive index of nanosheets or by the thermal effect of laser power. The absence of the SSPM pattern beyond the absorption band and diffraction patterns suggests that the observed change in refractive index is mainly due to thermal mechanisms. Based on our investigations, it is evident that the thermal effect has a significant influence on the interaction between intense light and samples. When a continuous wave laser is focused on a material, the absorbed energy of molecules and nanosheet particles causes the samples to heat up. Thermal conductivity enables the transfer of heat from the heated region to the surrounding areas, resulting in a non-local thermal effect. Our findings indicate that rGO/Hydraulic oil exhibits a higher nonlinear optical response compared to rGO-OH/Hydraulic oil and rGO-COOH/Hydraulic oil at the given wavelength, with nonlinear refraction indexes and thermo-optical coefficients at approximately 10^{-6} cm^2/W and 10^{-2} K^{-1}. respectively. The presence of derivatives of rGO significantly enhances the optical nonlinearity of hydraulic oil. The results of this study could provide new opportunities for advancing nonlinear optical applications, and they might open up new possibilities for the use of these materials in designing all-optical devices.

REFERENCES

[1] R.W. Terhune, P.D. Maker, and C.M. Savage, "Optical harmonic generation in calcite," Phys. Rev. Lett., Vol. 8, no. 10, pp. 404–406, 1962.

[2] P.A. Franken, A.E. Hill, C.W. Peters, and G. Weinreich, "Generation of optical harmonics," Phys. Rev. Lett., Vol. 7, no. 4, pp. 118–119, 1961.

[3] G.C. Righini and L. Sirleto, *Advances in nonlinear photonics*, Elsevier, 2023.

[4] Z. Chen and R. Morandotti, *Nonlinear photonics and novel optical phenomena*. Vol. 170, Springer, 2012.

[5] W.R. Callen, B.G. Huth, and R.H. Pantell, "Optical patterns of thermally self-defocused," Appl. Phys. Lett., Vol. 11, no. 3, pp. 103–105, 1967.

[6] X. Zhang, Z. Yuan, R. Yang, Y. He, Y. Qin, S. Xiao, and J. He, "A review on spatial self-

phase modulation of two-dimensional materials," J. Cent. South Univ., Vol. 26, no. 9, pp. 2295–2306, 2019.

[7] D.F. Eaton, "Nonlinear optical materials," Science, Vol. 253, no. 5017, pp. 281–287, 1991.

[8] C. Araujo, A.S.L. Gomes, and G. Boudebs, "Techniques for nonlinear optical characterization of materials: a review," Rep. Prog. Phys., Vol. 79, no. 3, pp. 036401–036401, 2016.

[9] Y. Wang, C. Y. Lin, A. Nikolaenko, V. Raghunathan, and E. O. Potma, "Four-wave mixing microscopy of nanostructures," Adv. Opt. Photon., Vol. 3, no. 1, pp. 1–52, 2010.

[10] E. Hendry, P.J. Hale, J. Moger, A. Savchenko, and S. Mikhailov, "Coherent nonlinear optical response of graphene," Phys. Rev. Lett., Vol. 105, no. 9, pp. 097401(1-4) 2010.

[11] P.B. Chapple, J. Staromlynska, J.A. Hermann, T.J. Mckay, and R.G. Mcduff, "Single-beam Z-Scan: measurement techniques and analysis," J. Nonlinear Opt. Phys. Mate.r, Vol. 6, no. 3, pp. 251–293, 1997.

[12] H. Zhang, S. Virally, Q. Bao, L. Kian Ping, S. Massar, N. Godbout, and P. Kockaert, "Z-scan measurement of the nonlinear refractive index of graphene," Opt. Lett., Vol. 37, no. 11, pp. 1856–1856, 2012.

[13] R. Wu, Y. Zhang, S. Yan, F. Bian, W. Wang, X. Bai, X. Lu, J. Zhao, and E. Wang, "Purely coherent nonlinear optical response in solution dispersions of graphene sheets," Nano Lett., Vol. 11, no. 12, pp. 5159–5164, 2011.

[14] W. Ji, W. Chen, S. Lim, J. Lin, and Z. Guo, "Gravitation-dependent, thermally-induced self-diffraction in carbon nanotube solutions," Opt. Express, Vol. 14, no. 20, pp. 8958–8958, 2006.

[15] A.N. Hassan, M.A. Haddad, M. Golestanifar, and A. Behjat, "Non-linear optical response as a food authentication: investigation of non-linear Optical Properties of Edible Oils by spatial self-Phase modulation (SSPM) method," Food Anal. Methods, Vol. 16, no. 8, pp. 1392–1402, 2023.

[16] M.D. Zidan, A.W. Allaf, A. Allaham, and A. AL-Zier, "Effect of sample position on formation of spatial-self phase modulation ring patterns in poly(azaneylylidene-acylene)," Optik, Vol. 283, pp. 170939–170939, 2023.

[17] W. Gao, S. Wang, J. Yuan, L. Xiao, S. Jia, and L. Wang, "Identification of orbital angular momentum using atom-based spatial self-phase modulation," Opt. Express, Vol. 31, no. 9, pp. 13528–13528, 2023.

[18] T. Neupane, B. Tabibi, W.J. Kim, and F. Jaetae Seo, "Spatial self-phase modulation in graphene-oxide monolayer," Crystals, Vol. 13, no. 2, pp. 271–271, 2023.

[19] Y. Shi, Y. Gao, Y. Hu, Y. Xue, G. Rui, L. Ye, B. Gu, "Spatial self-phase modulation with tunable dynamic process and its applications in all-optical nonlinear photonic devices," Opt. Lasers Eng., Vol. 158, pp. 107168–107168, 2022.

[20] L. Zhou, H. Fu, T. Lv, C. Wang, H. Gao, D. Li, L. Deng, and W. Xiong, "Nonlinear optical characterization of 2D materials," Nanomaterials, Vol. 10, no. 11, pp. 2263(1-38), 2020.

[21] T. Neupane, B. Tabibi, and F.J. Seo, "Spatial self-phase modulation in WS_2 and MoS_2 atomic layers," Opt. Mater. Express, Vol. 10, no. 4, pp. 831–831, 2020.

[22] E.A. Aboob and F.A. Umran, "Experimental study of spatial self-phase modulation (SSPM) based on laser beam and hybrid functionalized carbon nanotubes/silver nanoparticles (F-Mwcnts/Ag-Nps) acetone suspensions," Iraqi J. Laser, Vol. 18, no. 1, pp. 1-6, 2019.

[23] L. Ma, "Study on changes in spatial self-phase modulation pattern of graphene dispersion," J. Phys. Conf. Ser., Vol. 1838, no. 1, pp. 012021–012025, 2021.

[24] L. Ma, "Effect of convection on the distortion of spatial self-phase modulation pattern in graphene dispersions." J. Phys. Conf. Ser., Vol. 1838, no. 1, pp. 012002-012008, 2021.

[25] Y. Shan, J. Tang, L. Wu, S. Lu, X. Dai, and Y. Xiang, "Spatial self-phase modulation and all-optical switching of graphene oxide dispersions," J. Alloys Compd., Vol. 771, pp. 900–904, 2019.

[26] A.R. Sadrolhosseini, S. Abdul Rashid, H. Shojanazeri, M. Noor, and H. Nezakati, "Spatial self-phase modulation patterns in graphene oxide and graphene oxide with silver and gold nanoparticles," Opt. Quantum Electron., Vol. 48, no. 4, pp. 222-234, 2016.

[27] K.R. Vijesh, P.N. Musfir, T. Thomas, Manu Vaishakh, V.P.N. Nampoori, and S. Thomas,

"Enhanced nonlinear optical properties of solution dispersed carbon dots decorated graphene oxide with varying viscosity," Opt. Laser Technol., Vol. 121, pp. 105776–105776, 2020.

[28] Y. Yuan, B. Zhu, F. Cao, J. Wu, Y. Hao, and Y. Gu, "Enhanced nonlinear optical properties of the Cu_2Se/RGO composites," Results Phys., Vol. 27, pp. 104568(1-7), 2021.

[29] M. Yue, J. Si, L. Yan, Y. Yu, and X. Hou, "Enhanced nonlinear optical properties of reduced graphene oxide decorated with silver nanoparticles," Opt. Mater. Express, Vol. 8, no. 3, pp. 698–698, 2018.

[30] Y. Yuan, F. Cao, P. Li, J. Wu, B. Zhu, and Y. Gu, "Ultrafast charge transfer enhanced nonlinear optical properties of $CH_3NH_3PbBr_3$ perovskite quantum dots grown from graphene," Nanophoton., Vol. 11, no. 13, pp. 3177–3188, 2022.

[31] D. Berman, A. Erdemir, and A.V. Sumant, "Graphene: a new emerging lubricant," Materials Today, Vol. 17, no. 1, pp. 31–42, 2014.

[32] J. Zhao, J. Mao, Y. Li, Y. He, and J. Luo, "Friction-induced nano-structural evolution of graphene as a lubrication additive," Appl. Surf. Sci, Vol. 434, pp. 21–27, 2018.

[33] S. Zilabi, M. Shareei, A. Bozorgian, A. Ahmadpour and E. Esmaeil, "A review on nanoparticle application as an additive in lubricants," Adv. J. Chem. Sect. B. Nat. Prod. Med. Chem., Vol. 4, pp. 209-221, 2022.

[34] H.A. Naser, A. I. Mahmood, and S.K. Fandi, "Measurements of linear and nonlinear optical properties for iraqi heavy crude oil samples," Iraqi J. Science, Vol. 62, pp. 845–851, 2021.

[35] C.A. Emshary, D.H. Hashim, H.A. Sultan, and Q.M.A. Hassan, "Diffraction patterns and nonlinear optical properties of Henna oil," J. Pure Sci. Sci. Educ., Vol. 7, no. 4, pp. 90–103, 2017.

[36] A. Garcia, S. Valbuena, R. Sarmiento, and F. Racedo, "Measurement of the nonlinear optical properties of olive oil using Z-Scan," Opt. Pura Appl., Vol. 48, no. 1, pp. 55–61, 2015.

[37] J.S. Díaz-Tovar, S. Valbuena-Duarte, and F. Racedo-Niebles, "Study of non-linear optical properties in automobile lubricating oil via Z-Scan technique," Rev. Fac. Ingenieria., no. 86, pp. 27–31, 2018.

[38] R.F. Souza, Márcio A.R.C. Alencar, M.R. Meneghetti, and J.M. Hickmann, "Large nonlocal nonlinear optical response of castor oil," Opt. Mater., Vol. 31, no. 11, pp. 1591–1594, 2009.

[39] R.F. Souza, M.A.R. C. Alencar, M.R. Meneghetti, and J.M. Hickmann, "Nonlinear optical properties of castor oil." in Proc. advanced materials and structures, XXIX ENFMC, Annals of Optics, 2006.

[40] M.A.R.C. Alencar, C.M. Nascimento, S. Chávez-Cerda, M.G.A. da Silva, M.R. Meneghetti, J.M. Hickmann, "Large spatial self-phase modulation in castor oil enhanced by gold nanoparticles," in Proc. of SPIE, 2006,

[41] M. Izdebski, R. Ledzion, and P. Górski, "Measurement of quadratic electrogyration effect in castor oil," Opt. Commun., Vol. 346, pp. 80–87, 2015.

[42] D. S. Bolley, "Composition of castor oil by optical activity," J. Am. Oil. Chem. Soc., Vol. 30, no. 10, pp. 396–398, 1953.

[43] L. Vicari, "Optical nonlinearity in a film of water in oil microemulsion," Opt. Mater., Vol. 18, no. 1, pp. 155–157, 2001.

[44] L. Rosario, "Dynamics of optical nonlinearity in water-in-oil microemulsion," Jpn. J. Appl. Phys., Vol. 40, no. 2R, pp. 662–662, 2001.

[45] L. Vicari, "Laser beam self-phase modulation by a film of water-in-oil microemulsion," EPL., Vol. 49, no. 5, pp. 564–568, 2000.

[46] L. Vicari, "Optical nonlinearity of water in oil microemulsion near percolation," J. Appl. Phys., Vol. 88, no. 1, pp. 7–10, 2000.

[47] S.A. Sangsefedi, S. Sharifi, H.R. M. Rezaion, and A. Azarpour, "Fluorescence and nonlinear optical properties of alizarin red S in solvents and droplet," J. Fluoresc., Vol. 28, no. 3, pp. 815–825, 2018.

[48] F.A. Zarif, S. Sharifi, G.S. Shurshalova, I. Rakhmatullin, V. Klochkov, A. Aganov, M. Behrouz, M.R. Sharifmoghadam, S. Mahdizadeh, and M.K. Nezhad "Effect of micelles and reverse micelles on nonlinear optical properties of potassium dichromate and Staphylococcus aureus treatment," Opt. Mater., Vol. 106, pp. 109925–109925, 2020.

[49] S. Sharifi, S.G. Salavatovna, A. Azarpour, F. Rakhshanizadeh, G. Zohuri, and M.R. Sharifmoghadam, "Optical properties of

methyl orange-doped droplet and photodynamic therapy of staphylococcus aureus," J. Fluoresc., Vol. 29, no. 6, pp. 1331–1341, 2019.

[50] M. Pourtabrizi, N. Shahtahmassebi, A. Kompany, and S. Sharifi, "Enhancement of linear and non-linear optical properties of erythrosin b by nano-droplet," Opt. Quantum Electron., Vol. 50, no. 13, pp. 1-15, 2018.

[51] R. Barbosa-Silva, M.L. Silva-Neto, D. Bain, L. Modesto-Costa, T. Andrade-Filho, V. Manzoni, A. Patra, and C.B. de Araújo, "Observation and analysis of incoherent second-harmonic generation in gold nanoclusters with six atoms," J. Phys. Chem. A, Vol. 124, no. 28, pp. 15440–15447, 2020.

[52] J.W. You, S.R. Bongu, Q. Bao, and N.C. Panoiu, "Nonlinear optical properties and applications of 2D materials: theoretical and experimental aspects," Nanophotonics, Vol. 8, no. 1, pp. 63–97, 2018.

[53] K.S. Novoselov, D. Jiang, F. Schedin, T.J. Booth, V.V. Khotkevich, S.V. Morozov, and A.K. Geim, "Two-dimensional atomic crystals," in Proc. of the National Academy of Sciences, Vol. 102, no. 30, pp. 10451–10453, 2005.

[54] J.E.Q. Bautista, C.L.A.V. Campos, M.L. da Silva-Neto, C.B. de Araújo, A.M. Jawaid, Robert Busch, R.A. Vaia, and A.S.L. Gomes, "Intensity-dependent thermally induced nonlinear optical response of two-dimensional layered transition-metal dichalcogenides in suspension," ACS Photon, Vol. 10, no. 2, pp. 484–492, 2023.

[55] R.W. Boyd, *Nonlinear optics,* Academic Press, 2019.

[56] Y. Wang, Y. Tang, P. Cheng, X. Zhou, Z. Zhu, Z. Liu, D. Liu, Z. Wang, and J. Bao, "Distinguishing thermal lens effect from electronic third-order nonlinear self-phase modulation in liquid suspensions of 2D nanomaterials," Nanoscale, Vol. 9, no. 10, pp. 3547–3554, 2017.

[57] J.E.Q. Bautista, M.L. da Silva-Neto, C.L.A.V. Campos, M. Maldonado, C.B. de Araújo, and A.S.L. Gomes, "Thermal and non-thermal intensity dependent optical nonlinearities in ethanol at 800 nm, 1480 nm, and 1560 nm," J. Opt. Soc. Am. B, Vol. 38, no. 4, pp. 1104–1104, 2021.

[58] M.D. Zidan, M.M. Al-Ktaifani, M.S. EL-Daher, A. Allahham, and A. Ghanem, "Diffraction ring patterns and nonlinear measurements of the Tris(2′,2-bipyridyl) iron(II) tetrafluoroborate," Opt. Laser Technol., Vol. 131, pp. 106449–106449, 2020.

[59] K. Ogusu, Y. Kohtani, and H. Shao, "Laser-induced diffraction rings from an absorbing solution," Opt. Rev., Vol. 3, no. 4, pp. 232–234, 1996.

[60] "Thermal Conductivities for some common liquids," Engineeringtoolbox.com, 2019. https://www.engineeringtoolbox.com/thermal-conductivity-liquids-d_1260.html.

Moein Golestanifar earned his BSc in atomic physics from Yazd University in 2013. He is currently pursuing his MSc in Optics and lasers at Yazd University. He worked as a Master's student at the Laser Spectroscopy Research Laboratory (LSRL) in nonlinear optics from 2019 to 2021 at Yazd University.

Mohammad Ali Haddad received his Ph.D. in Atomic and Molecular Physics from VU-Amsterdam in 2014. He currently is the director of the Laser Spectroscopy Research Laboratory (LSRT) at Yazd University. His research interests include laser physics, applied spectroscopy, and nonlinear optics.

Amir Namiq Hassan received his MSc degree in optics and laser from Yazd University, Iran, in 2023. Currently, he works as a researcher at the University of Sulaimani, Kurdistan Regional, Iraq. His primary research interest lies in the nonlinear optical properties of various materials.

Fatemeh Ostovari received her Ph.D. in physics from the Tarbiat Modares University, Tehran, Iran, in 2014. Dr. Ostovari is an associate professor in the Department of Physics, Yazd University, Yazd, Iran, ever since. Her main interests include nano-optoelectronic, nanophysics, and nano-biophysics.